Epigallocatechin-3-gallate PEGylated poly(lactic-co-glycolic) acid nanoparticles mitigate striatal pathology and motor deficits in 3-nitropropionic acid intoxicated mice

Amanda Cano[a,b,c, #], Miren Ettcheto[c,d,e], Marta Espina[a,b], Carmen Auladell[f], Jaume Folch[c,e], Britta A. Kühne[d], Marta Barenys[d] , Elena Sánchez-López[a,b,c], Eliana B. Souto[g,h], Maria Luisa García[a,b,*], Patric Turowski[i,*], Antoni Camins[c,d,*]

[a] Department of Pharmacy, Pharmaceutical Technology and Physical Chemistry, Faculty of Pharmacy and Food Sciences, University of Barcelona, Spain.
[b] Institute of Nanoscience and Nanotechnology (IN2UB), Barcelona, Spain.
[c] Biomedical Research Networking Centre in Neurodegenerative Diseases (CIBERNED), Madrid, Spain.
[d] Department of Pharmacology, Toxicology and Therapeutic Chemistry, Faculty of Pharmacy and Food Sciences, University of Barcelona, Spain.
[e] Unit of Biochemistry and Pharmacology, Faculty of Medicine and Health Sciences, University of Rovira i Virgili, Reus (Tarragona), Spain.
[f] Department of Cellular Biology, Physiology and Immunology, Faculty of Biology, University of Barcelona, Spain.
[g] Department of Pharmaceutical Technology, Faculty of Pharmacy, University of Coimbra, Coimbra, Portugal.
[h] CEB - Centre of Biological Engineering, University of Minho, Campus de Gualtar 4710-057 Braga, Portugal.
[i] UCL Institute of Ophthalmology, University College of London, United Kingdom.

[*] **Senior co-authors.**

[#]**Amanda Cano**, Department of Pharmacy, Pharmaceutical Technology and Physical Chemistry, Faculty of Pharmacy and Food Sciences. Av Joan XXIII, 27-31, 08017. University of Barcelona, Barcelona, Spain.
E-mail address: acanofernandez@ub.edu

Financial support

This work was supported by the Spanish Ministry of Economy and Competitiveness (SAF2017-84283-R), CB06/05/0024 (CIBERNED) and the European Regional Development Founds. AC[a,b,c], ME[a,b], ESL[a,b,c] and MLG[a,b] belong to 2017SGR-1477. ME[c,d,e], CA[f], and AC[c,d] belong to 2017SGR-625.

Acknowledgements

Authors acknowledge the support of the Spanish Ministry of Science, Innovation and Universities, Biomedical Research Networking Centre in Neurodegenerative Diseases (CIBERNED) and European Regional Development Founds.

Key words

Epigallocatechin-3-gallate; polymeric nanoparticles; PLGA-PEG; 3-nitropropionic acid; Huntington's disease; neurodegenerative diseases.

Abbreviations

3-NP, 3-nitropropionic acid; AA, ascorbic acid; ASOs, antisense oligonucleotides; BWT, Beam walk test; DALYs, disability-adjusted life year; EE, encapsulation efficiency; EGCG, Epigallocatechin-3-gallate; FDA, Food and Drug Administration; FJC, Fluoro-Jade C; GFAP, glial fibrillary acidic protein; HD, Huntington's disease; *HTT*, Huntingtin; mHTT, mutant HTT protein; ND, neurodegenerative diseases; NPs, nanoparticles; NPCs, neuronal progenitor cells; OFT, open field test; OxHb, oxidized hemoglobin; PDI, polydispersity index; PEG, polyethylene glycol; PFA, paraformaldehyde; PLGA, poly (lactic-co-glycolic acid); TEM, transmission electron microscopy; TST, tail suspension test; XRD, X-ray diffraction; Z_{av}, mean average size; ZP, zeta potential.

Structured Abstract

Aims: To compare free and nanoparticle (NP)-encapsulated epigallocatechin-3-gallate for the treatment of Huntington's disease (HD)-like symptoms in mice.

Material and Methods: EGCG was incorporated into PEGylated PLGA NPs with AA. HD-like striatal lesions and motor deficit were induced in mice by 3-NP-intoxication. EGCG and EGCG/AA NPs were co-administered and behavioral motor assessments and striatal histology performed after 5 days.

Results: EGCG/AA NPs were significantly more effective than free EGCG in reducing motor disturbances and depression-like behaviour associated with 3-NP toxicity. EGCG/AA NPs treatment also mitigated neuroinflammation and prevented neuronal loss.

Conclusion: NP encapsulation enhances therapeutic robustness of EGCG in this model of HD symptomatology. Together with our previous findings, this highlights the potential of EGCG/AA NPs in the symptomatic treatment of neurodegenerative diseases.

Lay Abstract:

Huntington's disease (HD) is a debilitating neurodegenerative disease that affects around 5-10/100,000 individuals in developed countries. It is caused by genetic alterations in the huntingtin (*htt*) gene. Efforts are being made to find treatments which will correct the genetic alterations or their pathophysiological consequences associated with HD,

however none of these options are yet available to patients. Thus, therapies that address and ameliorate the symptomatology of HD, which include motor dysfunction and a wide range of behavioural disturbances, are also needed. Epigallocatechin-3-gallate (EGCG) is a powerful compound extracted from the green tea plant that may possess beneficial effects for HD patients, but whose therapeutic success is limited because of its chemical instability. Here, we show that protective encapsulation of EGCG rendered it much more efficient in attenuating motor deficits and depression-like behaviour in a mice model of HD-like neurodegeneration. Importantly, behavioural improvement was also associated with a reduction of neuronal damage. These results, together with our previous findings using nanoparticle-encapsulated EGCG in mouse models of Alzheimer's disease and epilepsy, highlight their potential effectiveness for symptomatic treatment of neurodegenerative diseases.

Graphical Abstract

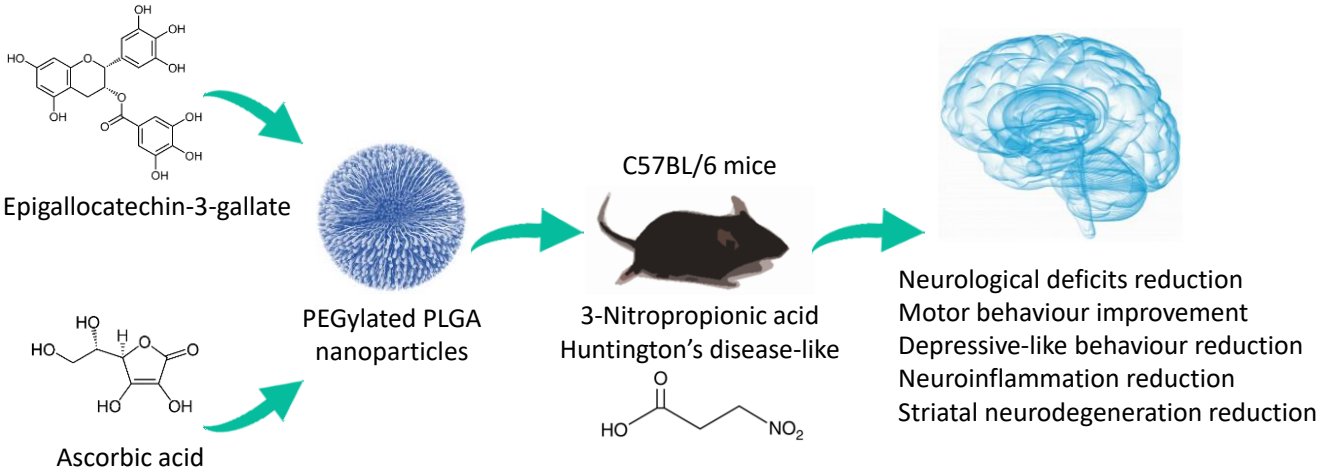

1. Introduction

Neurodegenerative diseases diseases are increasingly prevalent in developed countries [1]. Huntington's disease (HD), an autosomal neurodegenerative disease, is mainly characterized by a motor dysfunction accompanied by behavioural disturbances ranging from irritability, apathy to depression and cognitive decline [2]. Specifically in HD, a region of repetitive CAG trinucleotides in exon 1, which encodes a polyglutamine stretch normally varying between 6 and 35 in length, is expanded, resulting in polyglutamine stretches exceeding 38 repetitions and leading to varying degrees of HTT

protein misfolding [3]. Misfolded HTT often aggregates, forming insoluble amyloid-like deposits, which possess cytotoxic activity and eventually induce cell death. Although disease-causing *HTT* variants are expressed from birth in all tissues of all HD patients, only the nervous system is ultimately affected by this misfolded protein response and only in later stages of life [4]. The most affected brain area is the corticostriatal region, indicating that striatal neurons are disproportionally sensitive [5]. However, despite these mechanistic insights, the consequences of *HTT* polymorphisms and the normal physiological role of HTT remain poorly understood [6].

Currently, HD affects ca. 5-10/100,000 individuals in developed countries with recent rises potentially linked to an increase in mutation rates [7]. HD is a chronic pathology without cure, with affected individuals expected to survive for 15–20 years after the onset of first symptoms [8]. Current efforts to find an effective HD cure are still at the stage of pre-clincal or clinical testing. These include; HTT-lowering therapies with focus on reducing transcript or protein accumulation through the use of antisense oligonucleotides (ASOs) or siRNA; regulating homeostasis of mutant HTT protein by inhibiting aggregation or promoting the HTT clearance; and reducing neuroinflammation. Additionally, much research also focuses on finding symptomatic treatment of HD [9–12]. Indeed, the only two drugs currently approved by the *Food and Drug Administration* (FDA) for the treatment of HD belong to this latter therapeutic class. Both tetrabenazine and its deuterated derivative SD-809 (deutetrabenazine) suppress specific symptoms of HD, namely spasmodic involuntary movements, commonly known as “chorea”. However, they also lead to serious adverse effects, such as deterioration of pre-existing depressions in patients.[13].

Phytochemicals have potential for neuroprotection and neurodegenerative diseases [14]. In this regard, epigallocatechin-3-gallate (EGCG), which is its most abundant polyphenol constituent of the green tea plant *Camellia sinensis*, has attracted considerable interest in recent years [15]. Many beneficial effects of the green tea plant, *Camellia sinensis*, have been attributed to EGCG, which is its most abundant polyphenol constituent [16]. A number of hydroxyls groups and aromatic rings significantly contribute to the potent antioxidant activity of EGCG [16]. However, they are also responsible for the low physicochemical stability of EGCG, which, together with low

intestinal absorption, significantly reduces its bioavailability and thus currently compromises its promising therapeutic potential [17].

Nanosystems used to develop controlled drug delivery systems, include many types of vehicles, core matrices and particle sizes. Their most important characteristics are the ability to increase the physicochemical stability of encapsulated compounds, improve drugs solubility and bioavailability problems, sustained release, control their pharmacokinetic, reduction of adverse effects and targeting to a specific organ [18]. Currently, polymeric nanoparticles (NPs) are among the most explored vehicles in nanomedicine, specifically those composed of poly (lactic-co-glycolic acid) (PLGA) matrices [19,20]. Polymeric NPs can be formulated as nanospheres or nanocapsules, depending on the structural arrangement of the polymer. Nanocapsules have a liquid core surrounded by a polymer cover, whereas nanospheres are entirely composed of a polymeric matrix. Importantly, whereas the active, vectorised compound is dissolved in the liquid core of nanocapsules, it is dispersed in the intramatrix space or adsorbed on the surface of nanospheres [21]. Furthermore, PLGA NPs are frequently surface modified using polyethylene glycol (PEG), leading to improved aqueous solubility and reduced immunogenicity, which are both thought to contribute to lower rates of NP clearance and increased long term NPs stability [22].

We have previously shown that incorporation of ECGC into PEGylated PLGA nanoparticles improves bioavailability and effectiveness and renders it more effective in treating seizures in a mouse model of temporal lobe epilepsy [23]. Further improvement of this nanosystem is achieved by additional co-loading of the NPs with ascorbic acid (AA) [24]. Oral administration of such EGCG/AA NPs improves pharmacokinetics in the circulation and crucially higher EGCG levels in the brain of mice, resulting in improved therapeutic efficacy in a mouse model of Alzheimer's disease [24]. In light of this clear therapeutic potential of EGCG in attenuating neurodegeneration, it is noteworthy that ECGC also inhibits the aggregation of mHTT protein in a dose-dependent manner *in vitro*, and leads to morphological and behavioral improvements in transgenic HD flies [25]. Here, we tested if EGCG and EGCG/AA NPs have therapeutic benefit in mice intoxicated with 3-nitropropionic acid (3-NP). This mitochondrial toxin causes bilateral striatal lesions in the brain and has been extensively used to model HD- like motor deficit symptoms [26]. Collectively, our data showed that EGCG formulated in NPs was more

effective than free EGCG in correcting cellular and behavioural dysfunction in this mouse HD model.

2. Materials and Methods

2.1 Preparation of NPs

EGCG/AA NPs were prepared by double emulsion method and optimized with a central composite factorial design as previously described [24]. Briefly, the internal water phase (W_1) composed by 1 ml of MQ water with EGCG (Capotchem Hangzhou, P.R.China) and AA (Sigma Aldrich, Madrid, Spain) was emulsified with the organic phase, 1.5 ml of ethyl acetate containing a dissolved amount of PLGA-PEG 5% (O) (Evonik Co., Birmingham, USA). The simple emulsion (W_1/O) was obtained by an ultrasounds cycle (Ultrasounds probe Sonics&Materials, INC. Newtown, USA) at 37% amplitude during 30s. Then, 2 ml of the external water phase (W_2), composed by Tween®80 2.5% as surfactant (Sigma Aldrich, Madrid, Spain), were added to the simple W_1/O emulsion and subjected to an extra ultrasounds cycle at the same amplitude for 3 min to lead to the formation of the double emulsion (W_1/O/W_2). The entire procedure was carried out in an ice bath. Finally, 2 ml of an aqueous solution of 0.04% Tween®80 was added dropwise to stabilize the emulsion and the organic solvent was evaporated by stirring during 24 h (**Figure 1A**).

2.2 Transmission electron microscopy

Transmission electron microscopy (TEM) was used to confirm the morphological properties of the developed NPs. Samples were diluted (1:10) and fixed on the surface of activated copper grids (UV light). To visualize the particles, NPs were subjected to negative staining with uranyl acetate (2%). Images were taken on a Jeol 1010 microscope (Jeol USA, MA, USA).

2.3 X-ray diffraction

EGCG/AA NPs were ultracentrifuged (Optima® LE-BOK Ultracentrifuge, Beckman, USA) at 25,000 g, 15 ºC for 15 min, and the pellet dried and pulverized to obtain the dry powder samples.

X-ray diffraction (XRD) was used to evaluate the crystalline status of EGCG/AA NPs components. Pulverized samples were placed in polyester films and exposed to CuK”

radiation (45 kV, 40 mA, ʎ= 1.5418 Å) in a range (2θ) from 2 ºC to 60 ºC and a measuring time of 200 s per step.

2.4 Cellular in vitro assays

2.4.1 Hemolysis

Hemolysis tests were performed as described elsewhere [23]. Briefly, blood from C57BL/6 mice was extracted by maxillofacial puncture and collected in heparinized tubes. Samples were centrifuged at 4,000 rpm for 5 min and erythrocytes were re-suspended in 0.9 % NaCl. Then, triplicate samples of 1 ml of free EGCG or NPs formulations were incubated with 100 µl of erythrocyte suspensions for 30 min, 6 or 12 h in a shaking water bath at 37 ºC. Distilled water and 0.9% NaCl were used as positive and negative controls, respectively. Finally, oxidation of released hemoglobin (OxHb) was promoted by exposing samples to light and its absorbance was measured with a GE Healthcare Genequant 1300 spectrophotometer at 540 nm. Up to 10% of hemolysis was considered as non-toxic.

2.4.2 Cytotoxicity

The cytotoxicity of EGCG/AA NPs was evaluated in PC12 and GPNT cells, widely-used culture models for neuronal and brain microvascular endothelial cells, respectively [27,28]. Both naive and differentiated PC12 cells were used to account for potential differences in susceptibility between proliferative and differentiated states [29,30]. Differentiated and undifferentiated PC12, as well as confluent GPNTs were exposed to increasing concentrations of EGCG/AA NPs for 24 h. PC12 viability was measured by means of Alamar Blue assay (Promega) in a FluoStar Optima Plate Reader (BMG Labtech, USA) at 544/590 nm. GPNTs viability was analysed by measuring the absorbance of MTT reduction in a Safire microplate reader (Tecan, Reading, UK) at 540 nm.

2.5 In vivo tests

2.5.1 Animals, experimental groups and treatment schedule

Every effort was made to reduce the number of animals and minimize animal suffering. All procedures involving animals were conducted in strict accordance with the European Community Council Directive 86/609/EEC, EU Directive 2010/63/EU for

animal experiments, the procedures established by the Department d′Agricultura, Ramaderia i Pesca of the Generalitat de Catalunya and approved by the local ethical committee (University of Barcelona). Male C57BL/6 mice (6 weeks, 21–25 g) were purchased from Envigo© (Europe region, Spain). They were kept at 23 ºC with a 12 h light-dark cycle and had access to food and water *ad libitum*. 3-NP was used to induce HD-like symptoms [31,32]. After environmental adaptation, animals were randomly divided into four groups (with at least 8 mice per group): saline control group (CTRL), 3-NP control group (3-NP), 3-NP + free EGCG treated group (free EGCG) and 3-NP + EGCG/AA NPs treated group (EGCG/AA NPs). Mice were injected intraperitoneally (i.p.) with EGCG or EGCG/AA NPs (containing 50 mg/kg of EGCG) and 1 h later with 3-NP (70 mg/kg) (Sigma Aldrich, Madrid) every day for 5 days. Equal volumes of saline were injected in control groups. At the end of the treatments, behavioural tests were performed (**Figure S1 of Supplementary material**).

2.5.2 Beam walk test

Beam walk tests (BWT) were performed as described Babu *et al.* with some modifications [33]. Briefly, motor performance was assessed by measuring the ability of mice to traverse a horizontal wood beam (1 cm x 80 cm) suspended 50 cm above a padded surface. The day before the test, animals were allowed to cross the beam 3 times for training purposes. Maximum test time was 60 s. Latency to cross the beam, speed, distance travelled, immobility periods and falls were recorded.

2.5.3 Open field test

Open field tests (OFT) were conducted as described in previous studies [32]. Briefly, exploratory and spontaneous locomotor activities of mice were tested in the center of a 50 cm diameter platform surrounded by 30 cm walls. After allowing 5 min for the mice to adapt to the novel environment, motor activities were recorded during a 10 min session. The ambulation distance and mean speed was recorded using SMART V3.0 (Panlab Harvard Apparatus, Germany) video tracking system. The test area was thoroughly wiped with a cloth containing ethanol solution 70% after each session to prevent any bias from olfactory cues.

2.5.4 Tail suspension test

The tail suspension test (TST) was selected as a measure of depression-like behaviour [32,34]. Mice tail ends were fixed to a raised structure 50 cm from the ground

and animals were hung upside down such that their bodies were suspended during a six-min session. Immobility time was scored during the final 4 min of the session as the time that mice spent hanging in an immobile position without any desire to free themselves.

2.5.5 Neurological scoring (movement analysis)

Movement analysis was used to derive a neurological scoring as previously described Ludolph *et al.* [35]. Briefly, neurological deficits on day 5 were evaluated on a 0-4 scale as follows: normal behaviour (0), general slowness of displacement resulting from mild hind limb impairment (1), marked gait abnormalities and incoordination (2), hind limb paralysis (3), movement incapacity resulting from fore limb and hind limb impairment (4).

2.6 Ex vivo assays

2.6.1 Immunohistochemistry assay

At the end of treatments and behavioural assays, mice were sacrificed by i.p. injection of ketamine:xylazine (100 mg:10 mg/kg, respectively) and perfusion with PFA 4%. Brains were removed and maintained at 4 °C in a 30 % sucrose PFA solution until coronal sections of 20 µm of thickness were cut using a cryostat (Leica Microsystems, Wetzlar, Germany). Brain slices were subjected to immunohistochemistry as described elsewhere [23]. Primary polyclonal antibody against glial fibrillary acidic protein (GFAP) (1:1000; Dako Chemicals, Glostrup, Denmark) and secondary antibody AlexaFluor 594 goat anti-rabbit (Red, 1:1000; Life Technologies, Cambridge, UK) were used. Image acquisition was carried out using an epifluorescence microscope (BX41, Olympus, Germany) equipped with MercuryShortArc HBO™ 103 W/2 laser; Olympus DP70 camera; UPlanFI 20x/0.50 Ph1, UPlanFI 10x/0.30 Ph1 and Plan 4x/0.10 lenses; Olympus DP Controller 1.1.1.65 software).

2.6.2 Fluoro-Jade C histochemistry

Fluoro-Jade C (FJC) staining was performed to evaluate neurodegeneration as described elsewhere [36]. Briefly, brain slides were immersed in 0.06 g/l of $KMnO_4$ and transferred to the staining solution containing 0.1 % of acetic acid and 0.0001% of FJC for 30 minutes in the dark. Then, the slides were dried, submerged in xylene and mounted

on gelatin-coated glass with DPX mounting media. Samples were imaged using an epifluorescence microscope (Olympus BX61).

2.6.3 Nissl staining

Nissl staining has been widely used to detect neuronal degeneration in different models of HD [37,38]. Brain coronal sections (20 µm thick) were rinsed with PBS, transferred to gelatin-coated glass and air dried for 24 h. Subsequently, slides were hydrated by consecutive immersion in 90 % EtOH, 70 % EtOH, and distilled water before staining with cresyl violet 0.1%. Slides were then washed twice with distilled water and dehydrated by consecutive immersion in 70 %, 90% and 100 % EtOH, and then twice in xylene. Finally, slides were air dried and covered using DPX. Stained sections were analysed using an Olympus BX61 microscope and stained neuronal cells were manually counted in a double-blind setup.

2.7 Statistical analysis

All quantitative data were processed using GraphPad 6.0 Prism and analysed for normal distribution using the D'Agostino & Pearson omnibus normality test. For normally distributed data groups comparisons were performed by one-way ANOVA followed by Tukey post hoc tests. All other data was analysed by non-parametric one-way Kruskal-Wallis test followed by Dunn's multiple comparisons. Statistical significant difference was set at $P<0.05$ (*).

3. Results

3.1 Physicochemical characteristics of optimized EGCG/AA NPs formulation

EGCG/AA NPs were previously optimized, thus leading to a formulation composed by 2.5 mg/ml of EGCG, 2.5 mg/ml of AA and 14 mg/ml of PLGA-PEG [24]. This composition results in particles with an average size (Z_{av}) of 124.8 ± 5.2 nm, monodisperse population with a polydispersity index (PDI) of 0.054 ± 0.013 and a zeta potential (ZP) of -15.7 ± 1.7 mV. Such EGCG/AA NPs release almost 50% of the loaded drug in sustained fashion from the polymeric matrix at 24 h, and EGCG stability is significantly increased due to the incorporation of EGCG into the developed nanocarrier [24].

Additional TEM analyses showed that EGCG/AA NPs were perfectly spherical, possessed a smooth surface and did not display any aggregation phenomenon (**Figure 1B**). Moreover, the PEGylated cover was clearly identified by TEM (Figure 1B, inset). All physicochemical EGCG/AA NPs characteristics are summarized in **Table 1**.

The crystalline or amorphous state of substances is one of the physicochemical characteristics that strongly determines their biopharmaceutical behaviour. EGCG and AA displayed intense sharp peaks at diffraction angles, suggesting properties of both drugs typical of crystallization. Major XRD experimental peaks of 95% pure EGCG correlated with those obtained from literature [39] [experimental (literature)]: 5.13 (5.72), 8.46 (8.63), 10.30 (10.40), 12.09 (11.99), 17.00 (16.99), 20.70 (20.66), 24.51 (24.66), 29.47 (29.65). Free EGCG and AA showed XRD profiles of crystalline compounds. PLGA-PEG exhibited an amorphous pattern typical of copolymers. Empty and drug-loaded NPs displayed similar XRD profiles to PLGA-PEG polymer profile alone, indicating that new covalent bonds were not created between EGCG or AA and PLGA-PEG. Thus, these results demonstrate that both EGCG and AA were properly encapsulated inside the polymeric matrix, maintaining their crystallinity, and by inference, their effectiveness (**Figure 1C**).

3.2 Cellular viability assays

Hemolysis assays were performed and showed that both free and loaded-EGCG led to less than 10 % erythrocyte breakdown for assay times up to 12 h and free EGCG, AA and EGCG/AA NPs at concentrations up to 2.5 mg/ml (**Figure 2A, Table S1 of Supplementary material**). Brain endothelial GPNT cells treated with increasing concentrations of EGCG/AA NPs for 24 h remained viable, with only some insignificant reduction in cell viability at very high EGCG concentrations (450 µg/ml for 24 h). (**Figure 2B**). Undifferentiated PC12 showed no reduction in viability in presence of up to 300 µg/ml NP-formulated EGCG (**Figure 2C**). In contrast, when cultured under differentiating conditions, PC12 cells were more sensitive. Cell viability diminished in response to EGCG/AA NPs at concentration greater than 80 µg/mL. However, it never dropped below 50% within the concentration range tested and consequently, a half maximal inhibitory concentration (IC50) could not be determined.

3.3 EGCG/NPs ameliorated 3-NP-induced neurological deficits

Neurological deficits induced by 3-NP toxicity were evaluated by movement analysis. 3-NP resulted in clear motor abnormalities, with these mice displaying an average neurological score of nearly 3, corresponding to hind limb paralysis (**Figure 3A)**. These mice generally exhibited slowness, motor incoordination and common hind limb paralysis. Importantly, more than 50% of 3-NP mice exhibited score values higher than 3, with two of them being completely immobile. Treatment of 3-NP mice with free EGCG resulted in a significant improvement in the neurological score, with none of the treated animals showing any sign of hind limb paralysis or inability to move. EGCG/NP treatment was even more effective; this treatment group displayed a score value close to 0.

3.4 EGCG/AA NPs on 3-NP reduced depression-like behaviour

Time spent in immobility in the TST was used to evaluate potential depression. By this measure, as illustrated in **Figure 3B**, EGCG possessed a potent antidepressant effect in 3-NP HD-induced mice.

3.5 EGCG/AA NPs improved 3-NP induced motor disturbances

We used 3-NP intoxicated mice to model symptoms of HD and evaluate the effectiveness of EGCG to reduce associated motor disturbances. BWT and OFT are useful tests to evaluate motor skills, balance and fine coordination, and have been widely used to analyse motor alterations in a variety of different HD mouse models [31,40,41]. When subjected to a BWT assay, more than 55% of 3-NP mice fell from the beam, as opposed to none in the untreated control group (**Table 2**). None of the EGCG/AA NPs treated 3-NP mice exhibited any fall, either. **Figure 3C** shows the typical loss of gait posture observed in 3-NP mice and its absence in animals that were also treated with EGCG/AA NPs. Significantly, 3-NP mice took on average ca. 20 times longer to cross the beam than untreated littermates (**Figure 3D**). EGCG/AA NPs, but not free EGCG treatment significantly reduced crossing time; with average crossing times being close to those of control animals. The distance travelled on the beam was reduced ca. 2-fold in mice subjected to 3-NP but was within control values with animals treated with either free and NP-formulated EGCG (**Figures 3E**). 3-NP-treated mice also travelled at much reduced speed. In contrast, with EGCG/AA NPs but not free EGCG treatment these 3-NP mice travelled again at control speeds (**Figures 3F**). In summary EGCG/AA NPs treatment

significantly ameliorated performance of 3-NP mice in BWT. A clear improvement in agility of movements, coordination, body posture and gait, all very similar to those control littermates, was also observed as illustrated in the accompanying video (**Supplementary material**).

OFT, also frequently used to analyse motor disturbances in mice [42] confirmed our BWT observations. Intoxication with 3-NP led to significant reduction in the movement distance and speed of mice. EGCG/AA NPs treatment prevented these deficiencies, and significantly more so than free drug. (**Figure 3G, 3H**). All detailed data obtained in the behavioural tests are summarised in **Table 2**.

3.6 EGCG/AA NPs reduce astrogliosis

Neuroinflammation was evaluated by analysing astrocyte activation and concomitant enhanced GFAP expression by immunohistochemistry [43]. In both, the caudoputamen and hippocampal regions, 3-NP intoxication led to enhanced astrocyte reactivity, as well as changes in cell morphology, with dendritic alterations clearly evident (**Figure 4A)**. Both free and NPs-loaded EGCG administration reversed 3-NP-induced astrocyte reactivity in both brain regions. Whilst free EGCG did not normalize cell and dendrite morphology completely, EGCG/AA NPs treatment clearly did. Quantitative analysis confirmed that EGCG/AA NPs treatment significantly reduced the number of reactive astrocyte in 3-NP mice, not instead the free drug (**Figure 4B**).

3.7 EGCG/AA NPs reduce striatum neuronal death

FJC and Nissl staining were used as measures for neurodegeneration [38,44,45]. FJC showed that the brain area most affected by 3-NP intoxication was the dorsal striatum. Here, 3-NP mice clearly showed an intense FJC signal compared to control littermates, which barely displayed any sign of staining (**Figure 5A**). Both free and NPs-loaded EGCG treatments strongly reduced 3-NP-induced FJC staining. However, quantification of affected area showed that only EGCG/AA NPs appeared to be significant compared to those non-treated littermates.

Strong differences in Nissl brain staining between control and 3-NP-intoxicated mice were found in the lateral septral complex and the caudoputamen, both in frontal midbrain sections. As shown in **Figure 5B**, the total number of striatal neurons in Nissl-stained sections was significantly decreased in the 3-NP group. Brains of these animals

also displayed deformation of the neuronal body and dendrites, typical alterations of neuronal morphology associated with neurodegenerative processes [37,38,46,47] Striatal neuronal loss in 3-NP mice compared to control littermates ranged from between ca. 75% in the caudoputamen of midbrain sections to ca. 44 % and 48% in the caudoputamen and lateral septral complex of frontal brain sections, respectively. Free EGCG treatment was not able to significantly reduced 3-NP-induced neuronal loss in the analysed areas. Significantly, EGCG/AA NPs nearly completely prevented neuronal loss in the caudoputamen striatum, with neuronal cell loss completely absent and ca. 18% in in the caudoputamen of middle and frontal brain, respectively, and ca. 18% in the lateral septral complex of frontal brain (see also Supplementary **Table S2**).

4. Discussion

HD is a disabling ND caused by autosomal dominant mutations in the *HTT* gene that are related with nerve cell death. Despite this clear genetic link, there is no effective cure to date. Nevertheless, therapeutic strategies targeting the *HTT* gene and its expression are increasingly explored, with some at advanced stage. Currently, two types of ASOs are in clinical development for HD: the allele-specific ASOs, WVE-120101 (NCT03225833) and WVE-120102 (NCT03225846) and the non-allele specific ASO, IONIS HTTRx (NCT02519036) [8]. However, in line with many other ND, HD management and cures are generally recognised to require a multi-target approach, with those focusing on HD neurological symptoms continuing to be important, either as principal or adjunct treatment option [8].

Amongst phytochemicals, EGCG has increasingly drawn interest as a potential therapeutic due to its natural origin and its many beneficial properties [15]. In its free form, the therapeutic use of EGCG is limited because of limitation in bioavailability. Nevertheless, there is increasing evidence that EGCG may be beneficial for diseases without effective treatments and unclear etiology, such HD. Indeed, some studies have already evaluated the effect of EGCG in pre-clinical models of HD. Ehrnhoefer *et al.* carried out a study in an *in vitro* yeast model and transgenic flies of HD [25]. This study reported for the first time that EGCG can beneficially modulate HTT protein misfolding, resulting in a decrease of protein aggregation and cytotoxicity, and improvement of motor function. Likewise, Kumar and colleagues evaluated the effect of EGCG in 3-NP-intoxicated rats [48]. In this case, authors report that EGCG is able to restore the

glutathione system and improve memory processes. Lastly, in 2015 a phase II clinical trial of 12-month EGCG treatment in HD patients was initiated (NCT01357681). Its primary outcome evaluates changes of cognitive functions; however, results are not yet available.

Our study focused on EGCG loaded into PEGylated PLGA NPs under an antioxidant environment. Our previous studies show that the incorporation of EGCG into this nanocarrier results in an improvement of drug physicochemical stability and an enhanced EGCG bioavailability, as well as its sustained release from the polymeric matrix [24]. PEGylation of this polymer matrix and the use of Tween®80 as surfactant were specifically selected to develop these NPs since available evidence indicates that these components act as enhancers of NPs penetration to the brain [49,50]. Likewise, the biocompatibility, biodegradability, safety, easily elimination and surface modification versatility of PLGA provide a matrix with many advantages for the delivery of different drugs with widely different chemical characteristics in biomedical applications [51,52]. Our results here also demonstrated that the developed nanocarrier efficiently incorporates EGCG into the polymeric matrix, preserves the crystallinity properties of both drugs, and thus combined with a small Z_{av}, monodisperse population, high negative surface charge and elevated loading capacity give rise the appropriated characteristics for drug enhanced brain delivery.

EGCG/AA NPs did not display relevant cytotoxicity towards blood, neuronal and brain endothelial cells, and this was in full agreement with studies using similar nanocarriers [23,53]. In particular, the polymer on its own appears to have little effect on cells at the low concentrations present in vivo [24]. We also showed here that high concentrations of free or loaded EGCG, or empty NPs did not affect the integrity of red blood cells, again in line with previous studies [54–56]. No cytotoxicity of EGCG/AA NPs was detectable in cultured brain GPNT endothelial cells or undifferentiated PC12 neuronal cells. In accordance with results reported by Asaki *et al.* showing that differentiated PC12 are typically more sensitive [29], we found that differentiated PC12 exhibited some sensitivity towards EGCG/AA NPs. However, this was only seen at concentrations above 80 μg/ml ($p<0.05$); a concentration, which was never reached in vivo: even if all of the 50 mg/kg we injected i.p. into mice was in the circulation, this would translate to less than 1 mg/ml in the blood. We have previously shown that this

nanosystem does not accumulate in the brain at more than 1/1000 of the circulating concentration [24], i.e. in the present at 1 µg/ml as a theoretical maximum and well below any cytotoxicity seen in differentiated PC12 cells. This confirmed that EGCG can be safely used in a neuronal environment, with protective effects of EGCG in (6-OHDA)-induced Parkison's disease model in PC12 cells also previously reported[57].

We chose to assess the effectiveness of EGCG and EGCG/AA NPs in 3-NP intoxicated mice, which, whilst not faithfully reproducing the genetically driven pathology and aetiology of HD, have been used extensively to model striatal lesions and motor deficit reminiscent of HD [26,31,58]. Using this model, we were able to show for the first time that the prophylactic administration of EGCG significantly improved the motor performance of 3-NP intoxicated. Significantly, whilst treatment with free EGCG positively affected some measures of motor performance such as distance travelled in BWT and speed in OFT, it was the treatment with the NP-encapsulated EGCG, which led to normal motor behaviour in all measured parameters of BWT and OFT. Furthermore, we noted normalisation of behavioural traits associated with depression by treatment with both free and encapsulated EGCG. Previous studies have already shown the beneficial effects of EGCG on locomotion in different animal models. HD is categorized in a *less common neurological disorders* group, together with motor dystrophies, such Duchenne muscular dystrophy [59]. Thus, In 2012, Nakae and collaborators reported that oral administration of EGCG to *mdx* mice, a mild phenotype model of Duchenne muscular dystrophy, significantly increases the locomotor activities [60]. Other have also reported that chronic EGCG treatment improves motor performance in motor neurodegenerative diseases, such amyotrophic lateral sclerosis [61]. The present study adds to this body of evidence and, in addition, demonstrates clear therapeutic superiority of using EGCG stabilised and protected in a nanocarrier, such as in our EGCG/AA NPs.

In vivo results also showed a reduction of 3-NP-induced neurotoxicity in mice when EGCG was co-administered with the 3-NP. The presence of AA (used at 50 mg/kg in our experiments) may have also contributed to mitigating symptoms of 3-NP toxicity: a previous study shows that AA at 100 mg/kg protects somewhat from 3-NP-induced oxidative damage [62]. However, given the demonstrated and greater overall effectiveness of free EGCG [15] and AA-free EGCG NPs [23] in models of NDs, a direct neuroprotective effect of AA can probably be discounted in favour of its EGCG

stabilising function. Importantly, we found again that overall EGCG was significantly more effective when used formulated as EGCG/AA NPs. EGCG-enhanced brain function as suggested by our behavioural assays was correlated by cytological observation, since EGCG reduced 3-NP-induced astrogliosis and neurodegeneration in the hippocampus and the striatum. Furthermore, EGCG was clearly neuroprotective in the striatum. The involvement of striatum in motor functions, especially the caudoputamen region, is widely recognised, as well as the relation between striatal neuronal loss and HD motor impairment [63–65]. Accordingly, we observed reduced neurodegeneration in the caudoputamen and the lateral septral complex; most significantly when EGCG/AA NPs were used. Importantly, these cytological observations correlated well with improved motor performance observed in these mice. EGCG also protects motor neurons in other models, such a transgenic mice model of amyotrophic lateral sclerosis or cultures of rat spinal cords [66,67]. Overall our results show that neuroprotection through EGCG treatment translated into strongly improved motor behaviour in a rodent preclinical model of HD.

5. Conclusions

In summary, the current study adds to increasing evidence of significantly improved pharmacological effectivity of EGCG when co-loaded with AA into PLGA-PEG NPs. Indeed, NP encapsulation clearly renders EGCG more robust for *in vivo* application and thus EGCG/AA NPs will facilitate future pre-clinical studies assessing the effectiveness of this phytochemical in ND. In 3-NP-induced HD-like mice, EGCG/AA NPs effectively restored locomotor performance and overall neurological score. It also reduced depression-like behaviour, neuroinflammation and neurodegeneration. Our study did not elucidate if EGCG/AA NP affected *HTT* driven pathology; more elaborate genetic models are required for that. Nevertheless, our data highlighted the potential benefits of this novel NP formulation to manage neurological symptoms of HD and thus, we also propose that EGCG/AA NPs could be a novel and promising adjuvant for the symptomatic treatment of a wide range of ND, and HD in particular.

Summary Points

- Epigallocatechin-3-gallate (EGCG) is the most abundant polyphenol of the tea plant and has previously shown to possess beneficial effects in HD, but its therapeutic instability compromises its therapeutic success.
- We have previously demonstrated that the encapsulation of EGCG into PLGA-PEG nanoparticles (NPs) improved EGCG stability and penetration into the brain, as well as improve drug effectiveness in other ND.
- In this study, EGCG-loaded NPs were administered to 3-nitropropionic acid (3-NP)-intoxicated mice, an accepted animal model of HD, to evaluate the potential effectiveness of developed nanocarrier in this ND.
- EGCG-loaded NPs were significantly more effective than free EGCG in reducing motor disturbances, depression-like behaviour, neuroinflammation and striatal neuronal loss.
- Thus, we propose EGCG-loaded NPs as a promising therapeutic adjuvant in the management of HD symptomatology.

Conflict of interest

None of the authors have any conflicts of interest including any financial, personal or other relationships with other people or organizations. All authors have reviewed the contents of the manuscript being submitted, approved its contents and validated the accuracy of the data.

References

Reference note: indicated references are '*' – of interest and "**" – of considerable interest.

1. ****Wyss-coray T. Ageing, neurodegeneration and brain rejuvenation. *Nature*. 539(7628), 180–186 (2016).**

Comprehensive and well described explanation of neurodegeneration and its development.

2. Handley RR, Reid SJ, Patassini S, *et al.* Metabolic disruption identified in the Huntington ' s disease transgenic sheep model. *Nature Publishing Group*. 11(6:20681), 1–11 (2016).
3. Jiang Y, Chadwick SR, Lajoie P. Endoplasmic reticulum stress : The cause and

solution to Huntington' s disease ? *Brain Research*. 1648, 650–657 (2016).

4. Gövert F, Schneider S. Huntington's disease and Huntington's disease-like syndromes: an overview. *Curr Opin Neurol*. 26(4), 420–7 (2013).

5. Margulis J, Finkbeiner S. Proteostasis in striatal cells and selective neurodegeneration in Huntington ' s disease. *Front Cell Neurosci*. 8, 1–9 (2014).

6. Bates G, Dorsey R, Gusella J, *et al.* Huntington's disease. *Nat Rev Dis Primers*. 23(1), 15005 (2015).

7. Rawlins MD, Wexler NS, Wexler AR, *et al.* The Prevalence of Huntington' s Disease. *Neuroepidemiology*. 46, 144–153 (2016).

8. Mestre TA. Recent advances in the therapeutic development for Huntington's disease. *Parkinsonism and Related Disorders*. 59, 125–130 (2019).

9. Stahl CM, Feigin A. Medical, Surgical, and Genetic Treatment of Huntington Disease. *Neurol Clin.* 8(2), 367–378 (2020).

10. Shannon KM. Recent Advances in the Treatment of Huntington's Disease: Targeting DNA and RNA. *CNS Drugs.* 34(3), 219–228 (2020).

11. **Kumar A, Kumar V, Singh K, *et al.* Therapeutic Advances for Huntington's Disease. *Brain Sci.* 10(1), 43 (2020).

Global vision of recent findings in Huntington therapeutic approach.

12. Costa-Valadão PA, Santos KBS, Ferreira E Vieira TH, *et al.* Inflammation in Huntington's disease: A few new twists on an old tale. *J Neuroimmunol.* 348, 577380 (2020).

13. Frank S, Testa C, Stamler D, *et al.* Effect of Deutetrabenazine on Chorea Among Patients With Huntington Disease: A Randomized Clinical Trial. *JAMA.* 316(1), 40–50 (2016).

14. Khan A, Jahan S, Imtiyaz Z, *et al.* Neuroprotection: Targeting Multiple Pathways by Naturally Occurring Phytochemicals. *Biomedicines.* 8(8), 284 (2020).

15. *Chowdhury A, Sarkar J, Chakraborti T, Pramanik PK, Chakraborti S. Protective role of epigallocatechin-3-gallate in health and disease : A perspective. *Biomedicine et Pharmacotherapy*. 78, 50–59 (2016).

Comprehensive and well described explanation of epigallocatechin-3-gallate multifactorial benefits.

16. Singh BN, Shankar S, Srivastava RK. Green tea catechin , epigallocatechin-3-gallate (EGCG): Mechanisms , perspectives and clinical applications Catechin backbone. *Biochemical Pharmacology*. 82(12), 1807–1821 (2011).

17. Krupkova O, Ferguson SJ, Wuertz-kozak K. Stability of (−)-epigallocatechin gallate and its activity in liquid formulations and delivery systems. *The Journal of Nutritional Biochemistry*. 37, 1–12 (2016).

18. Yun Y., Lee B., Park K, Lafayette W. Controlled Drug Delivery: Historical perspective for the next generation. *J Control Release*. 219, 2–7 (2015).

19. **El-say KM, El-sawy HS. Polymeric nanoparticles : Promising platform for drug delivery. *International Journal of Pharmaceutics*. 528(1–2), 675–691 (2017).

Complete and well described explanation of polymeric nanoparticles as promising vectors for drug delivery.

20. Cano A, Sánchez-López E, Ettcheto M, *et al.* Current advances in the development of novel polymeric nanoparticles for the treatment of neurodegenerative diseases. *Nanomedicine (London)*. 15(12), 1239–1261 (2020).

21. Cano A, Espina M, García ML. Recent Advances on Antitumor Agents-loaded Polymeric and Lipid-based Nanocarriers for the Treatment of Brain Cancer. *Current Pharmaceutical Design*. 26(12), 1316–1330 (2020).

22. Soo J, Xu Q, Kim N, Hanes J, Ensign LM. PEGylation as a strategy for improving nanoparticle-based drug and gene delivery. *Advanced Drug Delivery Reviews*. 99, 28–51 (2016).

23. *Cano A, Ettcheto M, Espina M, *et al.* Epigallocatechin-3-gallate loaded PEGylated-PLGA nanoparticles: A new anti-seizure strategy for temporal lobe epilepsy. *Nanomedicine: Nanotechnology, Biology, and Medicine*. 14(4), 1073–1085 (2018).

Previous relevant findings of EGCG NPs effectiviness in other neurodegenerative diseases.

24. *Cano A, Ettcheto M, Chang J, *et al.* Dual-drug loaded nanoparticles of Epigallocatechin-3-gallate (EGCG)/ Ascorbic acid enhance therapeutic efficacy of EGCG in a APPswe / PS1dE9 Alzheimer' s disease mice model. *Journal of Controlled Release*. 301, 62–75 (2019).

Previous relevant findings of EGCG NPs effectiviness in other neurodegenerative diseases.

25. Ehrnhoefer DE, Duennwald M, Markovic P, *et al.* Green tea (2) -epigallocatechin-gallate modulates early events in huntingtin misfolding and reduces toxicity in Huntington ' s disease models. *Human Molecular Genetics*. 15(18), 2743–2751 (2006).

26. Chandra R, Reddy S, Reddy S, *et al.* Neuroprotective activity of tetramethylpyrazine against 3-nitropropionic acid induced Huntington ' s disease-like symptoms in rats. *Biomedicine & Pharmacotherapy*. 105, 1254–1268 (2018).

27. Waetzig V, Ri J, Cordt J, *et al.* Neurodegenerative effects of azithromycin in differentiated PC12 cells. *European Journal of Pharmacology*. 809, 1–12 (2017).

28. Dragoni S, Hudson N, Kenny B, *et al.* Endothelial MAPKs Direct ICAM-1 Signaling to Divergent Inflammatory Functions. *The Journal of Immunology*. 2(19), 4074–4085 (2017).

29. Asaki NS, Aba NB, Atsuo MM. Cytotoxicity of Reactive Oxygen Species and Related Agents Toward Undifferentiated and Differentiated Rat Phenochromocytoma PC12 Cells. *Biol. Pharm. Bull.* 24, 515–519 (2001).

30. Ekshyyan O, Aw TY. Decreased susceptibility of differentiated PC12 cells to oxidative challenge : relationship to cellular redox and expression of apoptotic protease activator factor-1. *Cell Death and Differentiation*. 12, 1066–1077 (2005).

31. Dhadde SB, Nagakannan P, Roopesh M, *et al.* Effect of embelin against 3-nitropropionic acid-induced Huntington' s disease in rats. *Biomedicine et Pharmacotherapy*. 77, 52–58 (2016).

32. Wang L, Wang J, Yang L, *et al.* Effect of Praeruptorin C on 3-nitropropionic acid induced Huntington' s disease-like symptoms in mice. *Biomedicine et Pharmacotherapy*. 86, 81–87 (2017).

33. Babu S, Vijayan R, Sekar S, Mani S. Simultaneous blockade of NMDA receptors and PARP-1 activity synergistically alleviate immunoexcitotoxicity and bioenergetics in 3- nitropropionic acid intoxicated mice : Evidences from memantine and 3- aminobenzamide interventions. *European Journal of Pharmacology*. 803, 148–158 (2017).

34. Chmielarz P, Kreiner G, Kuśmierczyk J, *et al.* Depressive-like immobility behavior and genotype × stress interactions in male mice of selected strains in male mice of selected strains. *The International Journal on the Biology of Stress*. 3890, 1–8 (2016).

35. Ludolph A, He F, Spencer P, Hammerstad J, Sabri M. 3-Nitropropionic acid-exogenous animal neurotoxin and possible human striatal toxin. *Canadian Journal of Neurological Sciences*. 18(4), 492–498 (1991).

36. Gu Q, Schmued LC, Sarkar S, Paule MG, Raymick B. One-step labeling of degenerative neurons in unfixed brain tissue samples using Fluoro-Jade C. *Journal of Neuroscience Methods*. 208(1), 40–43 (2012).

37. Turmaine M, Raza A, Mahal A, Mangiarini L, Bates GP, Davies SW. Nonapoptotic neurodegeneration in a transgenic mouse model of Huntington ' s disease. *PNAS*. 97(14), 14–18 (2000).

38. Lallani SB, Villalba RM, Chen Y, Smith Y, Chan AWS. Striatal Interneurons in Transgenic Nonhuman Primate Model of Huntington ' s Disease. *Nature Scientific Reports*. 9(1), 3528 (2019).

39. Bureau I. Polymorphs of cocrystals of epigallocatechin gallate and caffeine (W O 2017 / 040809). 2(12), [PATENT REGISTRATION] (2017).

40. Carter RJ, Morton AJ, Dunnett SB. Motor Coordination and Balance in Rodents. *Current Protocols in Neuroscience*. 8(12), 1–14 (2001).

41. Luong TN, Carlisle HJ, Southwell A, Patterson PH. Assessment of Motor Balance and Coordination in Mice using the Balance Beam. *Journal of Visualized Experiments*. 10(49), 2376 (2011).

42. Seibenhener ML, Wooten MC. Use of the Open Field Maze to Measure Locomotor and Anxiety-like Behavior in Mice. *Journal of Visualized Experiments*. , e52434 (2015).

43. Hanisch U, Kettenmann H. Microglia : active sensor and versatile effector cells in the normal and pathologic brain. *Nature neuroscience*. 10(11), 1387–1394 (2007).

44. Ehara A, Ueda S. Application of Fluoro-Jade C in Acute and Chronic Neurodegeneration Models : Utilities and Staining Differences. *Acta Histochem Cytochem*. 42(6), 171–179 (2009).

45. Gutiérrez IL, González-Prieto M, García-Bueno B, Caso JR, Leza JC, Madrigal JLM. Alternative Method to Detect Neuronal Degeneration and Amyloid b Accumulation in Free-Floating Brain Sections With Fluoro-Jade. *ASN Neuro Methods*. 10, 1–7 (2018).

46. Loh DH, Kudo T, Truong D, Wu Y, Colwell CS. The Q175 Mouse Model of Huntington ' s Disease Shows Gene Dosage- and Age-Related Decline in Circadian Rhythms of Activity and Sleep. *PLOS ONE*. 8(7), 1–13 (2013).

47. Cicchetti F, Saporta S, Hauser RA, *et al.* Neural transplants in patients with Huntington ' s disease undergo disease-like neuronal degeneration. *PNAS*. 106(30), 12483–12488 (2009).

48. Kumar P, Kumar A. Effect of lycopene and epigallocatechin-3-gallate against 3-nitropropionic acid induced cognitive dysfunction and glutathione depletion in rat : A novel nitric oxide mechanism. *Food and Chemical Toxicology*. 47(10), 2522–2530 (2009).

49. Nance EA, Woodworth GF, Sailor KA, *et al.* A Dense Poly(ethylene glycol) Coating Improves Penetration of Large Polymeric Nanoparticles within Brain Tissue. *Sci Transl Med*. 4(149), 1–19 (2012).

50. Sun W, Xie C, Wang H, Hu Y. Specific role of polysorbate 80 coating on the targeting of nanoparticles to the brain. *Biomaterials*. 25, 3065–3071 (2004).

51. Zhang K, Tang X, Zhang J, *et al.* PEG – PLGA copolymers : Their structure and structure-in fl uenced drug delivery applications. *Journal of Controlled Release*. 183, 77–86 (2014).

52. Sharma S, Parmar A, Kori S, Sandhir R. PLGA-based nanoparticles : A new paradigm in biomedical applications. *Trends in Analytical Chemistry*. 80, 30–40 (2016).

53. Sánchez-lópez E, Ettcheto M, Egea MA, *et al.* New potential strategies for Alzheimer' s disease prevention : pegylated biodegradable dexibuprofen nanospheres administration to APPswe / PS1dE9. *Nanomedicine: Nanotechnology, Biology, and Medicine*. 13(3), 1171–1182 (2017).

54. Moses K, Pepple D, Singh P, Moses K, Pepple D, Singh P. The Protective Effect of Epigallocatechin-3-gallate on Paraquat-induced Haemolysis of Erythrocyte Membrane. *West Indian Med J*. 64(3), 186–188 (2015).

55. Raval JS, Fontes J, Banerjee U, Yazer MH, Mank E, Palmer AF. Ascorbic acid improves membrane fragility and decreases haemolysis during red blood cell storage. *Transfusion Medicine*. 23, 87–93 (2013).

56. Martins LG, Rubiana NM khalil, Mainardes M. PLGA Nanoparticles and Polysorbate-80-Coated PLGA Nanoparticles Increase the In vitro Antioxidant Activity of Melatonin. *Current Drug Delivery*. 15(4), 554–563 (2018).

57. Nie G, Cao Y, Zhao B. Protective effects of green tea polyphenols and their major

component, (-)-epigallocatechin-3-gallate (EGCG), on 6-hydroxydopamine-induced apoptosis in PC12 cells. *Redox Rep*. 7, 171–177 (2002).

58. Hoshi A, Tsunoda A, Yamamoto T, Tada M, Kakita A. Increased neuronal and astroglial aquaporin-1 immunoreactivity in rat striatum by chemical preconditioning with 3-nitropropionic acid. *Neuroscience Letters*. 626, 48–53 (2016).

59. Feigin VL, Abajobir AA, Abate KH, *et al.* Global , regional , and national burden of neurological disorders during 1990 – 2015: a systematic analysis for the Global Burden of Disease Study 2015. *Lancet neurology*. 16, 877–897 (2017).

60. Nakae Y, Dorchies OM, Ritter C, Ruegg UT. Quantitative evaluation of the beneficial effects in the mdx mouse of epigallocatechin gallate , an antioxidant polyphenol from green tea. *Histochem Cell Biol*. 137, 811–827 (2012).

61. Koh S, Mok S, Young H, *et al.* The effect of epigallocatechin gallate on suppressing disease progression of ALS model mice. *Neuroscience Letters*. 395, 103–107 (2006).

62. Rodríguez-Martínez E, Rugerio-Vargas C, Rodríguez AI, Borgonio-Pérez G, Rivas-Arancibia S. Antioxidant effects of taurine, vitamin C, and vitamin E on oxidative damage in hippocampus caused by the administration of 3-nitropropionic acid in rats. *Int J Neurosci.* 114(9), 1133–1145 (2004).

63. Isomura Y, Takekawa T, Harukuni R, *et al.* Reward-Modulated Motor Information in Identified Striatum Neurons. *The Journal of Neuroscience*. 33(25), 10209–10220 (2013).

64. *Guo Z, Rudow G, Pletnikova O, *et al.* Striatal neuronal loss correlates with clinical motor impairment in Huntington's disease. *Mov Disord*. 27(11), 1379–1386 (2012).

Comprehensive and well described explanation of the relation between striatal neuronal loss and Huntington's diseases motor disturbances.

65. Morigaki R, Goto S. Striatal Vulnerability in Huntington's Disease: Neuroprotection Versus Neurotoxicity. *Brain Sciences*. 7, 63 (2017).

66. Xu Z, Chen ÆS, Li ÆX, Luo G, Li ÆL, Le ÆW. Neuroprotective Effects of (-) -Epigallocatechin-3-gallate in a Transgenic Mouse Model of Amyotrophic Lateral Sclerosis. *Neurochem Res*. 31, 1263–1269 (2006).

67. Yu J, Jia Y, Guo Y, *et al.* Epigallocatechin-3-gallate protects motor neurons and regulates glutamate level. *FEBS Letters*. 584(13), 2921–2925 (2010).

Tables

Table 1. Physicochemical characteristics of optimized formulation of EGCG/AA NPs.

Compound	Chemical structure	Molecular weight (g/mol)	Concentration (mg/ml)	EGCG/AA NPs physicochemical characteristics		EGCG/AA NPs morphological characteristics
EGCG	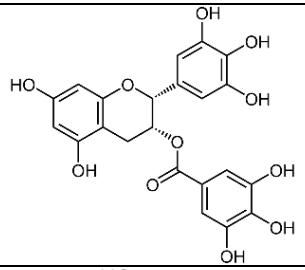	458,372	2.5	**Z_{av}**	124.8 ± 5.2 nm	Spherical shape, smooth surface, well defined PEG cover.
AA	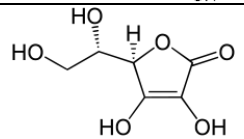	176,12	2.5	**PI**	0.054 ± 0.013	
PLGA-PEG	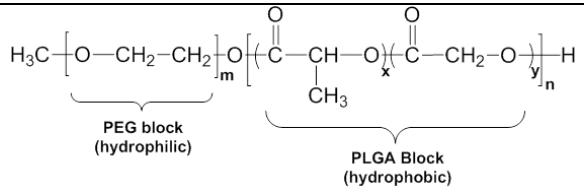	80.2 kDa	14	**ZP**	-15.7 ± 1.7 mV	
Tween®80	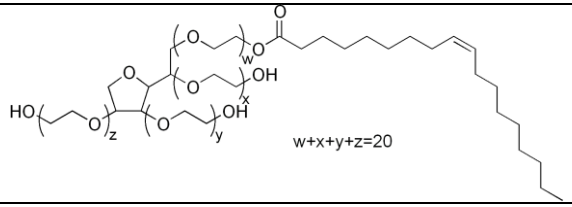	1.310	1.016 %	**EE_{EGCG}**	97.1 ± 2.4 %	
				EE_{AA}	94.3 ± 1.6 %	

Table 2. Behavioural test results of EGCG/AA NPs treatment of 3-NP-induced HD mice.

Behavioural test	Analysed conditions	Experimental groups			
		CTRL (n=8)	**3-NP (n=12)**	**Free EGCG (n=10)**	**EGCG/AA NPs (n=10)**
Beam walk	Falls	0	7	2	0
	Time for crossing (sec)	3.857 ± 0.806	25.262 ± 14.796	26.239 ± 6.693	9.950 ± 7.998
	Distance (cm)	80.0 ± 0.0	41.8 ± 29.0	69.1 ± 12.3	79.7 ± 1.1
	Speed (cm/sec)	21.4 ± 3.4	3.2 ± 2.4	3.0 ± 1.9	15.1 ± 6.0
Open field	Total distance (cm)	3161.9 ± 445.1	1143.9 ± 567.9	2146.9 ± 659.8	2936.9 ± 795.8
	Speed (cm/sec)	5.2 ± 0.7	1.9 ± 0.9	3.5 ± 1.1	4.9 ± 1.3
	Time at border (sec)	290.813 ± 36.340	397.198 ± 125.067	266.653 ± 84.793	199.87 ± 47.757
Tail suspension	Immobility (sec)	99.9 ± 31.8	165.5 ± 43.0	99.9 ± 38.2	90.5 ± 31.1
Neurological scoring	Score 0-4	0.000 ± 0.000	2.788 ± 0.958	1.600 ± 1.039	0.333 ± 0.497

Figures

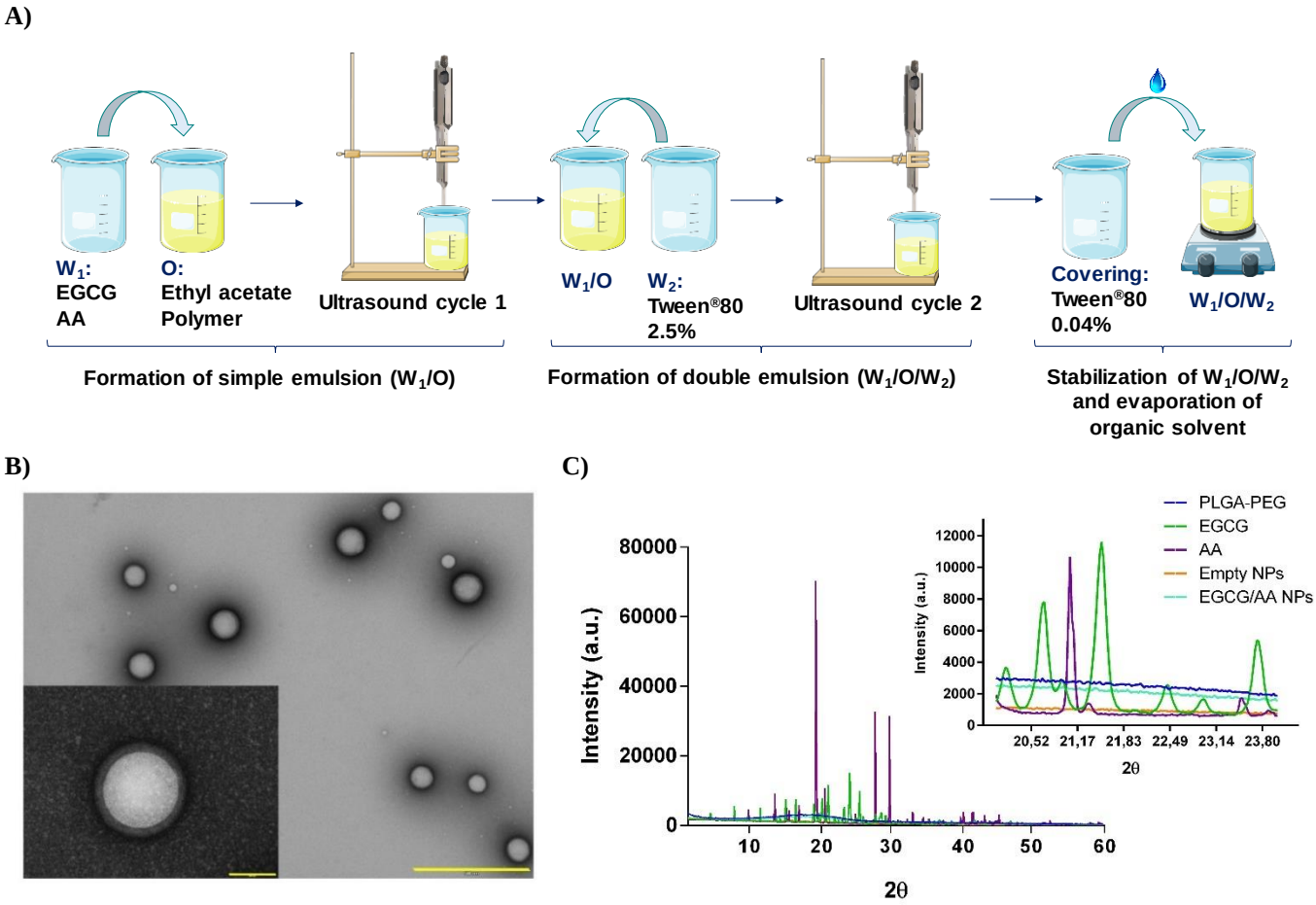

Figure 1. **EGCG/AA NPs preparation method and additional physicochemical characterization. (A)** Scheme of preparation of EGCG/AA NPs by the double emulsion method. Polymeric matrix: PLGA-PEG; loaded drugs: EGCG and AA; Surfactant: Tween®80. **(B)** EGCG/AA NPs morphology as revealed by TEM Scale bars 100/500 nm. **(C)** XRD profiles of different components of EGCG/AA NPs formulation, including an expanded view on the right of the 20 θ to 30 θ region.

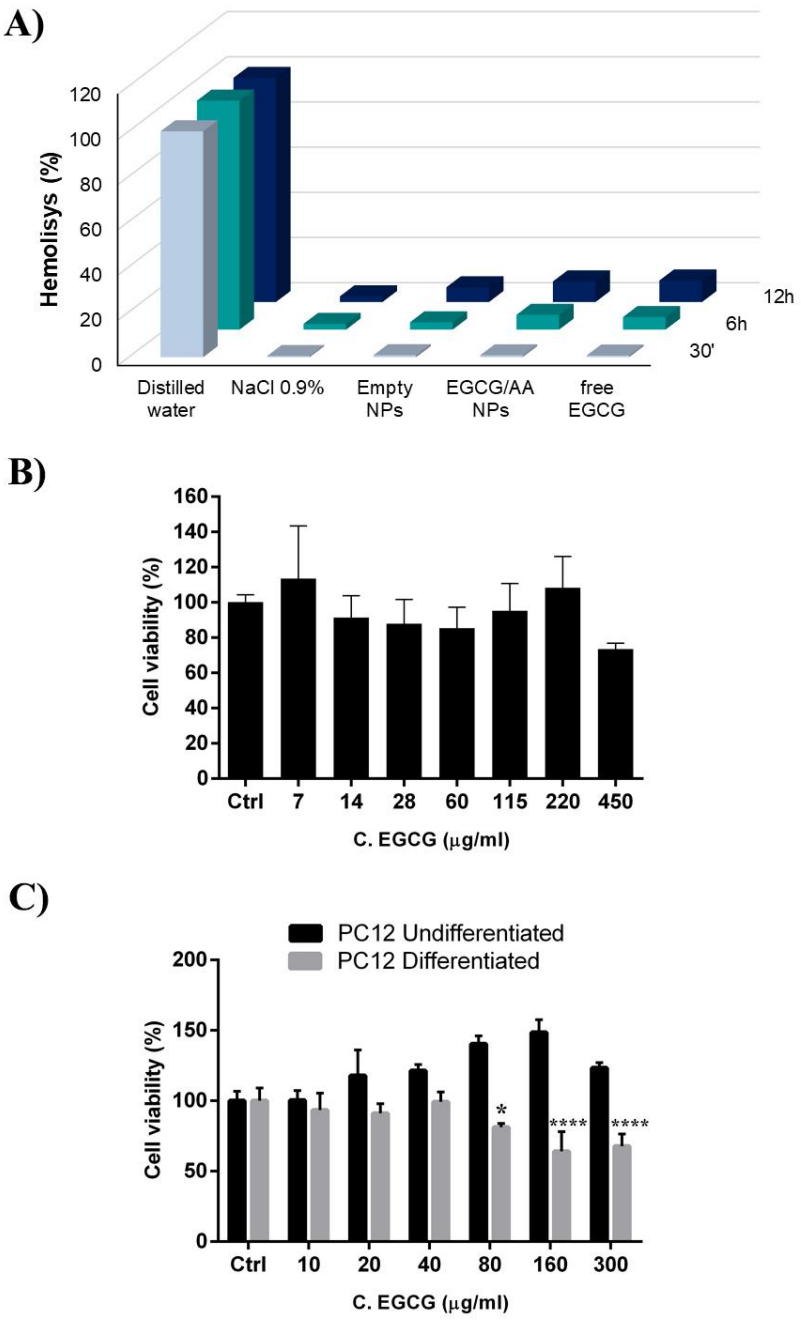

Figure 2. **Cell viability in response to EGCG/AA NPs**. **(A)** Hemolysis test results of EGCG/AA NPs and their constituents. Absorbance of released OxHb from erythrocytes was used to quantify hemolysis. Final concentrations of compounds were: EGCG/AA NPs: 2.5 mg/ml of EGCG, 2.5 mg/ml of AA and 14 mg/ml of PLGA-PEG; Empty NPs: 14 mg/ml of PLGA-PEG; free EGCG: 2.5 mg/ml **(B)** Cytotoxicity of EGCG/AA NPs measured by MTT assay in GPNT brain endothelial cell line. Cells were treated for 24 h with increasing amount of EGCG/AA NPs. Cell viability is expressed as a function of final EGCG concentrations (added as EGCG/AA NPs). Shown are normalised mean ± SD (n=3). **(C)** Cytotoxicity of EGCG/AA NPs measured by Alamar Blue assays in differentiated and undifferentiated PC12 neuronal cells. Cell viability is expressed as a function of final EGCG concentration (added as EGCG/AA NPs). Shown are normalised mean ± SD (n=3). One-way ANOVA statistical analysis followed by Bonferroni's multiple comparison test was performed. Statistical significance is expressed as $p<0.05$ *; $p<0.0001$ ****.

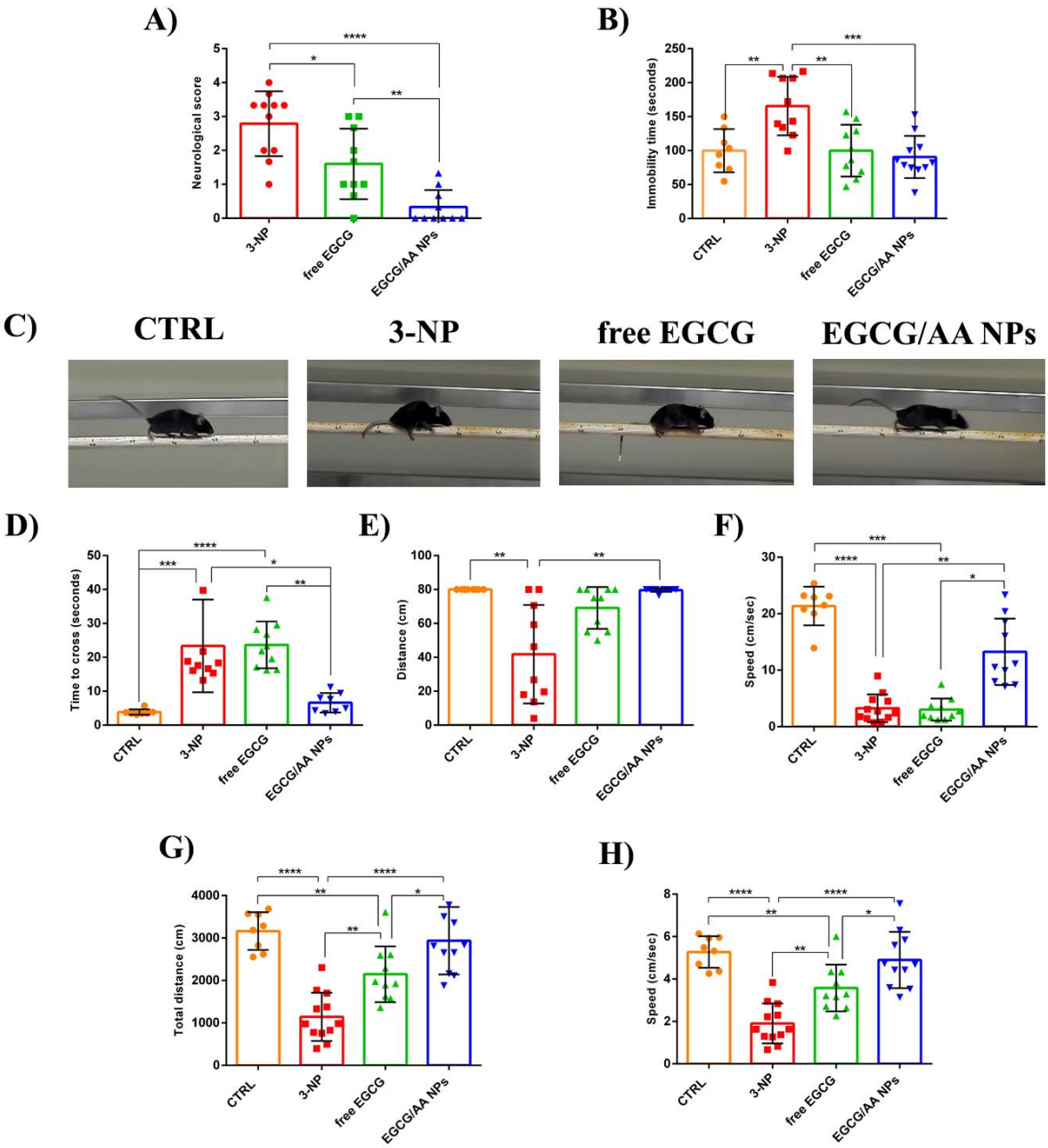

Figure 3. **Behavioural tests in 3-NP intoxicated mice and effect of EGCG**. 2 months-old C57BL/6 mice were i.p. injected daily with free and loaded EGCG (50 mg/kg/day) and with 3-NP (70 mg/kg/day) during 5 days. **(A)** Neurological score of the different experimental groups. **(B)** Time spent immobile in TST by the different experimental groups. **(C-F)** Assessment of animals by BWT. Typical gait posture of different groups in the BWT **(C)**. Quantification of time spent by animals to cross the complete beam **(D)**; of the total travel distance **(E)**, and of the mean speed **(F)** of different experimental groups in BWT. **(G-H)** Assessment by OFT results. Shown are the total travel distance **(G)** and the mean speed **(H)** of different experimental groups. One-way ANOVA statistical analysis followed by Tukey post hoc test was performed for panels **A, B, G** and **H.** One-way Kruskal-Wallis non-parametric statistical analysis followed by a Dunn's multiple comparisons test was performed for panels **D-F.** Statistical significance is expressed as $p<0.05$ *; $p<0.01$ **; $p<0.001$ ***; $p<0.0001$ ****.

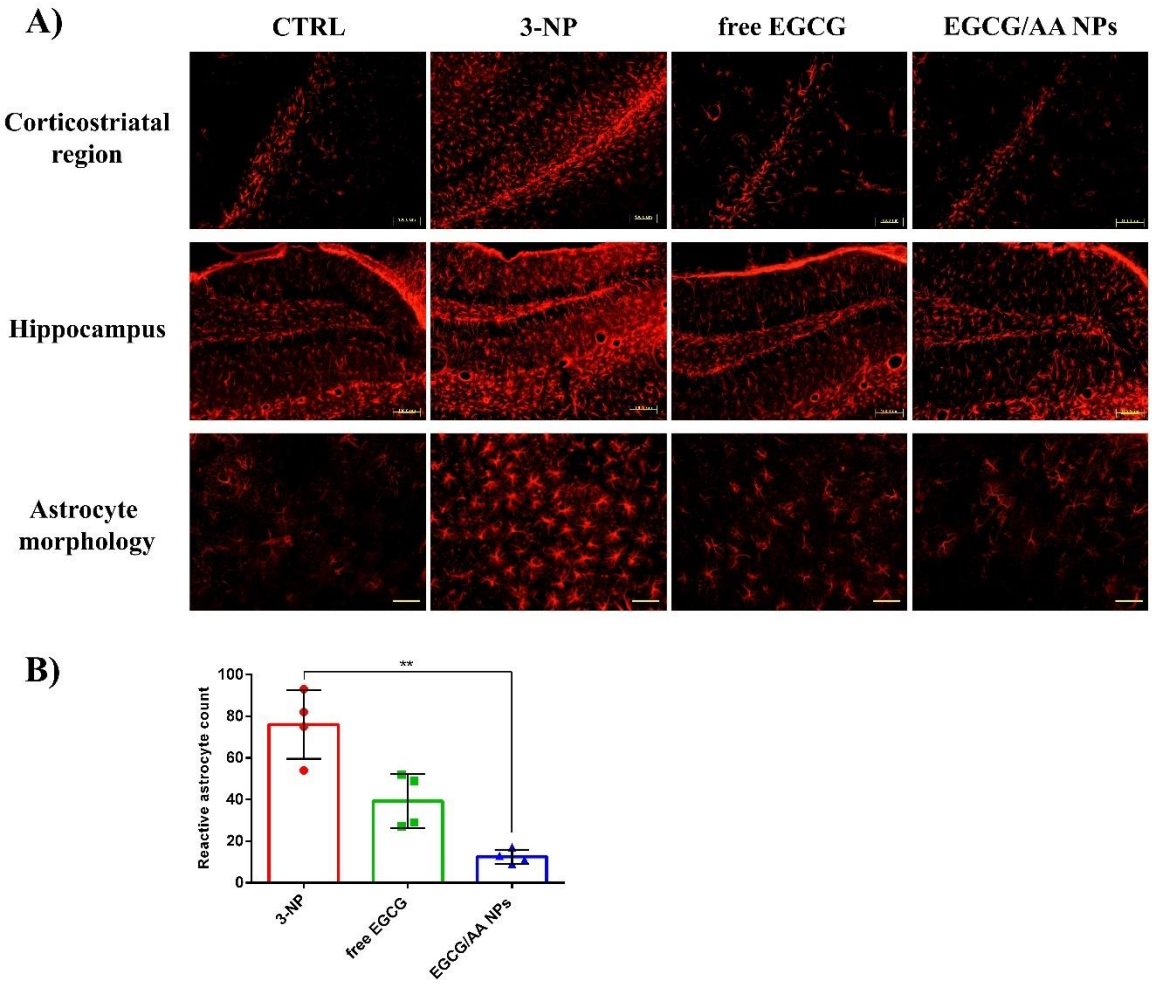

Figure 4. Astrogliosis in 3-NP intoxicated mice and effect of EGCG. 3-NP intoxication and EGCG treatments were performed as described for Figure 3. At the end of day 5, animals were sacrificed by perfusion with 4% PFA and brains were sectioned. GFAP immunostaining was performed on 20 µm coronal sections. **A)** *Dentate gyrus* of hippocampus and corticostriatal region are shown. Scale bar 100 µm. The bottom panels show astrocyte morphology of corticostriatal region of different experimental groups. Scale bar, 50 µm. (n=4/group). Images of each series have been acquired using identical settings. **B)** Quantitative analysis of reactive astrocytes in corticostriatal brain region of the different experimental groups. Analysis performed from images of corticostriatal region with scale bar of 50 µm. (n=4/group). One-way Kruskal-Wallis non-parametric statistical analysis followed by a Dunn's multiple comparisons test was performed for panel **B.** Statistical significance is expressed as $p<0.01$ **.

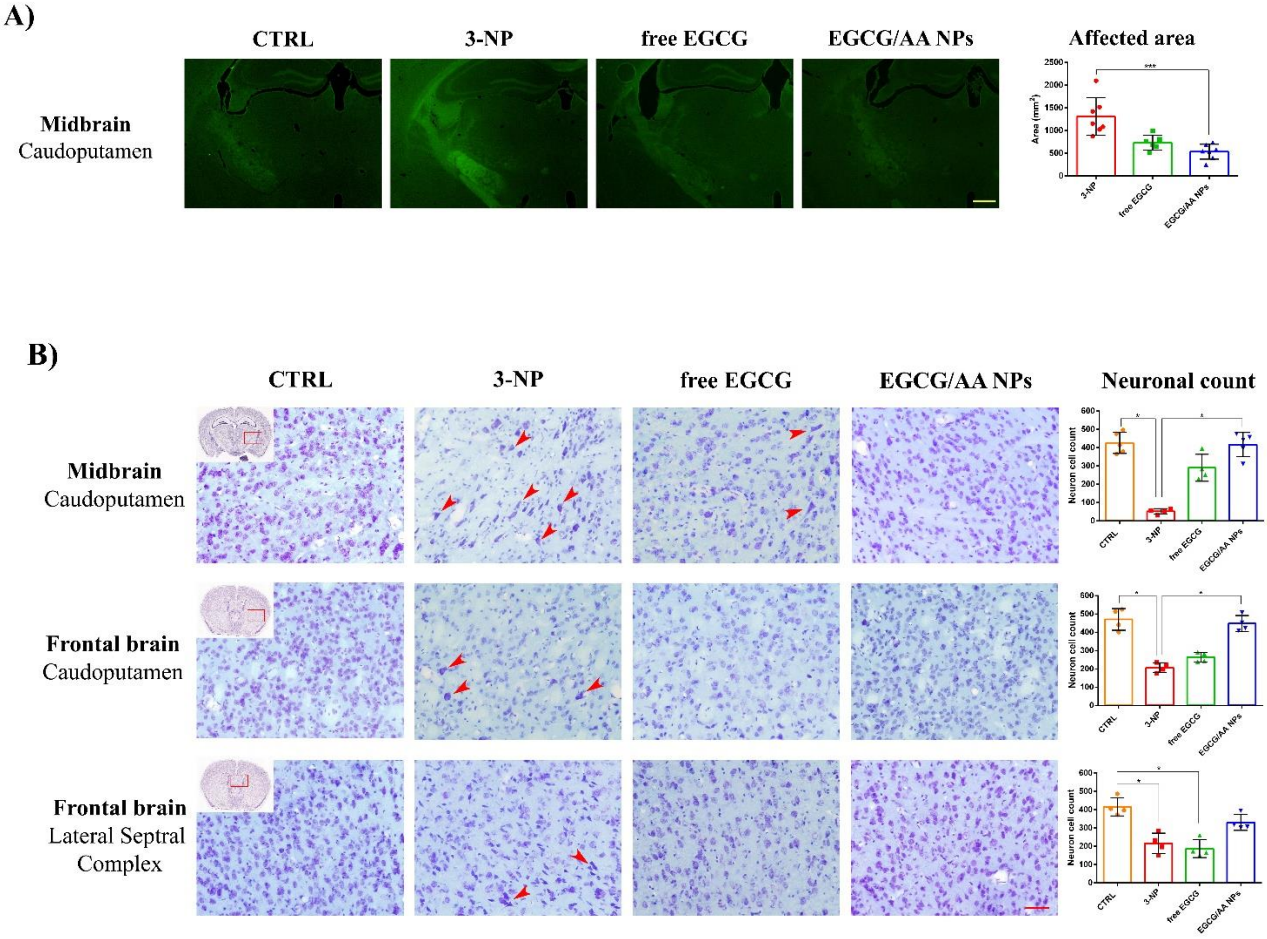

Figure 5. Effect of free and loaded EGCG on 3-NP-induced neurodegeneration. (A) As described for Figure 4, except that coronal sections were stained using FJC. Caudoputamen area of midbrain section are shown. Scale bar, 500 µm. Images of each series have been acquired using identical settings. Shown on the right is the quantification of FJC staining area as normalised mean cell count ± SD (n=6/group). **(B)** As described for Figure 4, except that Nissl staining was performed on 20 µm coronal sections. Striatal areas of frontal and midbrain section are shown. Red arrows point out morphological alterations of stained cells. Scale bar, 50 µm. Images of each series have been acquired using identical settings. Shown on the right are the quantifications of mean neuronal cell counts ± SD (n=4/group). One-way Kruskal-Wallis non-parametric statistical analysis followed by a Dunn's multiple comparisons test was performed for all quantifications in panels A and B. Statistical significance is expressed as $p<0.05$ *.